34th Annual International Conference of the IEEE EMBS
San Diego, California USA, 28 August - 1 September, 2012

Detecting flash artifacts in fundus imagery

Vincent C. Paquit[1], Ph.D., *Member, IEEE*, Thomas P. Karnowski[1], Ph.D., *Member, IEEE*, Deniz Aykac[1], *Member, IEEE*, Yaqin Li[2], Ph.D., *Member, IEEE*, Kenneth. W. Tobin[1], Jr., Ph.D., *Fellow, IEEE*, Edward Chaum[2], M.D., Ph.D., *Member, IEEE*

***Abstract*— In a telemedicine environment for retinopathy screening, a quality check is needed on initial input images to ensure sufficient clarity for proper diagnosis. This is true whether the system uses human screeners or automated software for diagnosis. We present a method for the detection of flash artifacts found in retina images. We have collected a set of retina fundus imagery from February 2009 to August 2011 from several clinics in the mid-South region of the USA as part of a telemedical project. These images have been screened with a quality check that sometimes omits specific flash artifacts, which can be detrimental for automated detection of retina anomalies. A multi-step method for detecting flash artifacts in the center area of the retina was created by combining characteristic colorimetric information and morphological pattern matching. The flash detection was tested on a dataset of 5218 images representative of the population. The system achieved a sensitivity of 96.54% and specificity of 70.16% for the detection of the flash artifacts. The flash artifact detection can serve as a useful tool in quality screening of retina images in a telemedicine network. The detection can be expected to improve automated detection by either providing special handling for these images in combination with a flash mitigation or removal method.**

I. INTRODUCTION

Since 2005 our team is pursuing the development of the Telehealth Retinal Image Analysis and Diagnosis (TRIAD) network [1]. This system, installed in walk-in clinics in the Mid-South of the United States of America, provides on-site assistance for image acquisition and pre-screening of diabetic retinopathy and associated conditions. Retinal images captured with fundus cameras go through (1) an image quality check to validate the data acquisition phase [2], (2) various feature extraction algorithms to identify and describe morphological characteristics associated with retinal abnormalities [3]–[5]. and provide real-time diagnostics, and finally (3) the image processing results and disease state are archived for later comparison with a diagnosis by an ophthalmologist. The automated diagnosis system currently does not replace screening by an eye specialist. We are investigating additional pre-processing techniques to increase our systems performance, and one problem we face is the presence of illumination artifacts that may cause flaws in our decision system. In this paper we present an original technique to find and delineate artifacts that were not detected by our image quality check algorithm. The paper is organized as follow: first we explain what flash artifacts are and how they affect the image, then we present our multi-phase approach to detect them, and finally we provide performance results.

II. FLASH ARTIFACTS

In general, artifacts commonly found in fundus images result from (1) foreign objects present in the field-of-view, (2) motion blur, (3) out-of-focus effect, and/or (4) extreme illumination conditions. In all of these cases, the whole image is usually affected and therefore it is trivial to detect them. As part of the TRIAD framework, we are always processing newly captured images with an image quality check algorithm before releasing them for further processing. In general, most of these artifacts are detected early in the process. However, there are also illumination artifacts affecting the image locally that cannot be detected with a global evaluation of the images. These artifacts can be located anywhere in the images, but a common one is an annular artifact in the middle of the fundus images, which often corresponds to the macula region. Annular artifacts are characteristic of the acquisition system configuration which combines the fundus camera and an annular source to ensure adequate illumination of the retina. Depending on changing combinations of data acquisition parameters (focus, exposure, field-of-view, etc.) and retinal pigmentation characteristics, these artifacts of varying intensity strengths appear superimposed on the fundus images, changing the local topography and to some extent are impacting the ability to analyze accurately the retina. To illustrate the annular illumination patterns we want to detect, an example of four

Fig. 1. Examples of flash artifacts: all four images are altered by an annular flash artifact. One can see that the intensity of the artifact combined with the retina pigmentation produces visible differences. Also, sometimes the annular artifact is not visible to the eye (see image on the far right) but its presence, detected by image processing algorithms, can impact detection and/or classification results.

These studies were supported in part by grants from Oak Ridge National Laboratory, the National Eye Institute, (EY017065), by an unrestricted UTHSC Departmental grant from Research to Prevent Blindness (RPB), New York, NY, by The Plough Foundation, Memphis, TN and by the Regional Burgundy Council, France. This manuscript has been authored by Oak Ridge National Laboratory, Oak Ridge, TN, USA, operated by UT-Battelle, LLC, under contract DE-AC05-00OR22725 with the US Department of Energy.

[1]V.C.Paquit (paquitvc@ornl.gov), T.P.Karnowski, D.Aykac, K.W.Tobin Jr. are with the Oak Ridge National Laboratory, Oak Ridge, TN 37831 USA.

[2]Y.Li and E.Chaum are with the University of Tennessee Health Science Center, Memphis TN 38163 USA.

central regions cropped out from larger images are given in Figure 1.

III. METHOD

In this section we describe the workflow of our image processing approach which includes contrast enhancement, annular artifact detection, and artifact delineation. At this stage it is important to note that we are only interested in detecting the central annular flash artifact or ring, therefore in the following we will be working only with pre-defined regions-of-interest. Going though the image database and only considering images where the ring was clearly visible, we noticed that size and shape of the artifact were fairly consistent and that the center of the ring was only slightly shifted from the center of the image. Therefore we have made the empirical choice to define our region-of-interest (ROI) as a 256×256 pixels area centered in the middle of the image.

A. Contrast enhancement

Fundus images are color images in the sRGB color space presenting variations in terms of hue, intensity, and contrast resulting from a combination of patient specific retina pigmentation (often associated with the patients ethnicity) and quantity of light entering the eyeball (associated with the pupil dilation diameter). Exploiting these particularities, segmentation techniques analyze images projected from the sRGB color space into another color space (HSV or CIE L*C*h* for example) or are using dimension reduction techniques such as PCA and LDA to increase the data variability in order to help with feature extraction and pixel classification [6]. Unfortunately, for our application these approaches are extremely unstable due to the important variations in terms of intensity and color of the artifact pattern, and classification results were unreliable. Consequently instead of using projection techniques for classification purpose, we used them to create contrast enhanced images suitable to perform topographic pattern matching. Amongst all the techniques we have tested, we identified two complementary methods to extract interesting contrast enhanced images of flash artifacts. Looking closely at the initial color ROIs, one notices that the ring is mainly visible in the green and blue channel and almost invisible in the red channel (see Figure 2). We have focused our approach on the blue channel because the ring visibility was more consistent in that channel. Therefore, our first image transformation consists of estimating the "blueness" of the color image, which is almost equivalent to computing the normalized RGB color channel except we maximize the blue channel response by imposing $I(x, y, blue) = 1$ for the denominator as formulated with Equation 1:

$$B(x, y) = \frac{I(x, y, blue)^2}{I(x, y, red)^2 + I(x, y, green)^2 + 1} \quad (1)$$

where B is the contrast enhanced image created based on blueness, I is the captured image, (x, y) is the two-dimensional image coordinate, and $\{red, green, blue\}$ are the color channels. Results obtained for five images from the database are presented Figure 2, second column. The second transformation converts a color image into a grayscale image while preserving hue information:

$$G(x, y) = I_\omega(x, y) + \lambda C_\omega(x, y) \quad (2)$$

where G is the grayscale contrast enhanced image, I_ω is the captured image represented with weighted components, (x, y) is the two-dimensional image coordinate, C_ω is the weighted chrominance component, and λ is the amount of chrominance applied to the intensity value. The complete mathematical formulation of this transformation is complex, therefore we strongly encourage interested readers to refer to

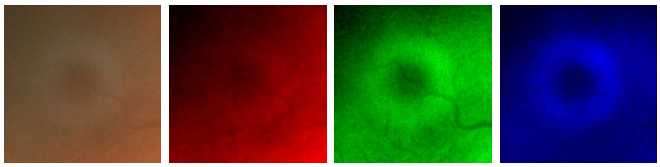

Fig. 2. Example image and channels: (left) input color image, (R,G,B images) normalized independent channels. We can see that the ring is not visible in the red channel but is visible in the blue channel and also in the green channel. It is actually a special case to show to illustrate which channel is mainly impacted by the flash artifact and also to point out that even in the best case scenario, the blue channel has more potential than the green channel.

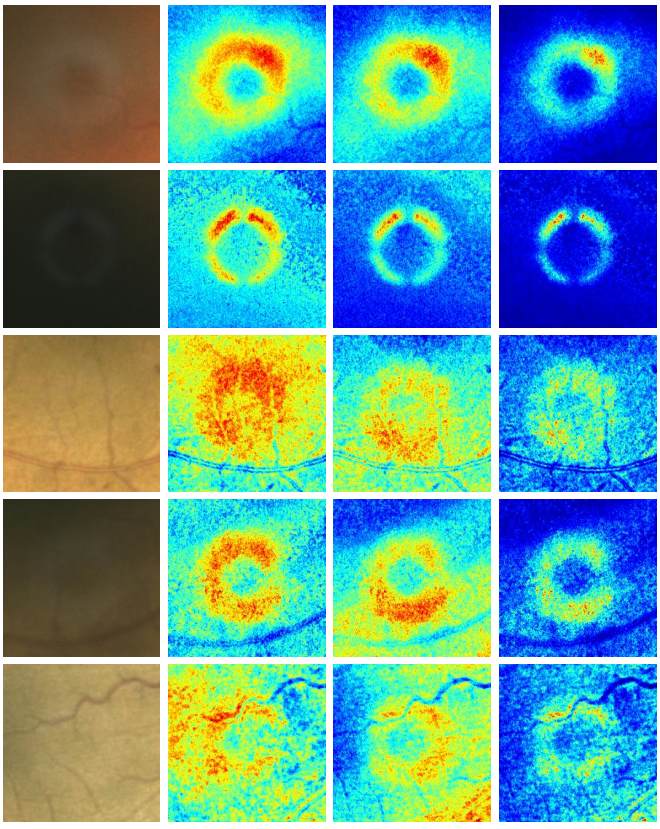

Fig. 3. Contrast enhancement results: (from left to right) input images, contrast enhancement using Equation 1, contrast enhancement using Equation 2, combination of both result for improved image enhancement. Contrast enhanced images (values ranging from 0 to 1 on a single channel) are displayed with a jet colormap for visualization purpose.

[7] for further details. With this transformation, one obtains a grayscale patchwork of isoluminant colors as one can see Figure 3, third column. Independently, both methods have average performances. However once combined together by computing the direct product between both results, the contrast enhanced images were visually better in the sense that they were showing a clear difference between the area impacted by the annular artifact and the rest of the image, see Figure 3, fourth column.

B. Ring detection

The images presented in Figure 3 show various morphological characteristics of the images present in our database: (1) ring artifact has a diameter approximately equal to half the size of the ROI; (2) its position can be slightly shifted from the center of the ROI; (2) the thickness is not constant (thin if the artefact projection is focused on the retina, wide if it is out of focus). An obvious solution is to apply a Hough transform with a circle as a primitive to find all circles present in the image [8], and select only two that best delineate the inside and outside of the ring. However, the success of the operator greatly depends on the sharpness of the artifact and on its intensity, two conditions that are not robust for all the images. Therefore a more suitable approach is to locate approximately the ring position with an image registration technique based on image cross-correlation [9]. By computing the cross-correlation between a reference image and the fundus images, one obtains a peak corresponding to the maximal correlation. The location of this peak is then used to estimate the 2D rigid translation between both images. Our reference image is a synthetic binary image the same size as the ROI, with a black background and a white ring on its center. The ring diameter is about half the size of the ROI and its thickness is equal to 5% of the diameter. In order to more accurately represent the smoothed edges of the ring a Gaussian filter (kernel size = 15 pixels) is applied to the image. There is a unique reference image to process the entire database, since the objective of this registration phase is not to detect the artifact accuratly but to detect if the ring is present and approximate its location in the ROI. The exact detection of all pixels part of the artifact is done in the following step. Figure 4 gives examples of registration results.

C. Delineation of the flash artifact

The ring detection algorithm gives a good approximation of the ring position. However, since it is a rigid pattern matching method, any changes in scaling or ring thickness will not be detected. Our first approaches to improve the artifact delineation were based on region growing algorithms (connected component, snake, etc.) and probabilistic methods [8], but none of them was stable, due to the lack of energy and the SNR of the artifact pattern area. Therefore we opted for a morphological approach widely used in 3D imaging called Iterative Closest Point (ICP) algorithm [10] which aims to find the transformation between a point cloud and a reference surface, respectively in our case between the detected ring and the contrast enhanced image. The original ICP formulation is a rigid transformation that finds optimal rotation and translation, therefore there will be minimal improvements in comparison to the previous cross-correlation approach. However, by using finite difference methods, it is also possible to solve for resize and shear [11]. Both the shifted reference image and the input image are converted into two sets of 3D points by considering the intensity values as z coordinates, the (x, y) pairs being the pixels coordinates in each image. It is important to notice that only non zero element of the reference image will be converted in a 3D point cloud, and that a pre-positioned reference

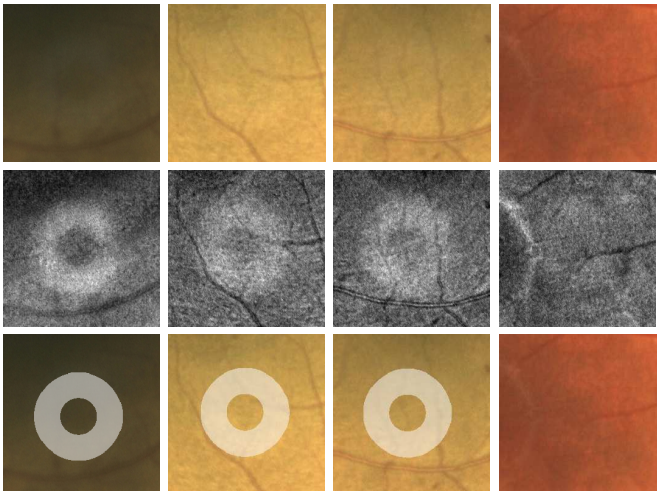

Fig. 4. Examples of ring detection results: (top) input images, (middle) contrast enhanced image showing computed with the method presented in sub-section III-A, (bottom) input image with the mask approximating the position of the detected ring overlaid on it. Notice that the ring is not always located in the centre and that no ring was detected for the last image because none was present.

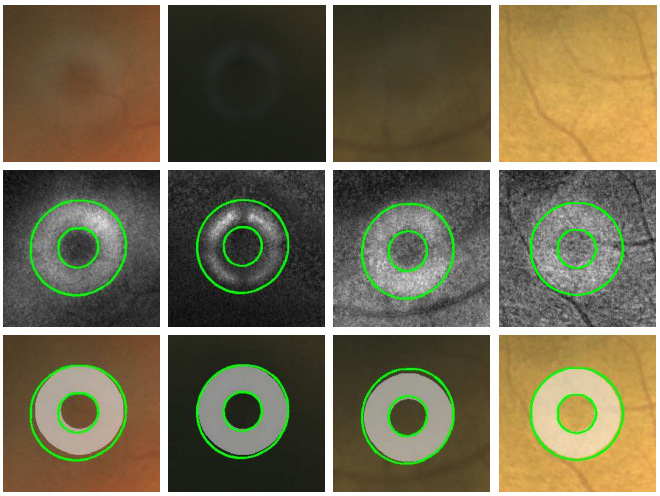

Fig. 5. Result of the flash artifact delineation: (top) input images, (middle) contrast enhanced image computed with the method presented in sub-section III-A; the green ellipses correspond to the inner and outer limit of the detected ring after ICP, (bottom) input image with overlaid on it the initial initial approximation of the ring (white) and in green the final delineated area obtained after mesh to mesh fitting using ICP.

image is required since the ICP algorithm needs a good starting point to avoid being trapped in a local minima. By applying the ICP algorithm, the reference image of the ring will slowly fit to the artifact pattern and cover it, giving a better approximation of the area impacted by the flash artifact. This fitting phase is not critical in our process of identifying if a ring artifact if present or not. However it is an intermediary step needed prior to any local analysis of the detected area and it also justify our approach toward the next phase of this research.

IV. EXPERIMENT

A. Dataset

Our dataset includes 5,218 retina fundus images collected from February 2009 to August 2011 from several clinics in the mid-South region of the USA as part the TRIAD telemedical project. The images represented both healthy and abnormal retinas and have color variations covering the normal pigmentation spectrum found in the patient population, which is approximately 70% African American and 30% Caucasian.

B. Performance

We applied our techniques to the entire database, recorded all intermediary results and validated manually the ring artifact detection and delineation results. For this purpose we use a GUI showing the original image, the contrast enhanced image, and having two selectors to tag each image with two labels: first, the visible presence of the ring was identified as *not present*, *not visible*, *barely visible* or *visible*; second, the accuracy of the detection was arbitrary qualified as correct if the detected area was (1) centered on the ring, and (2) covering most of the ring, otherwise it was marked as incorrect. If the ring was not visible in the original image, the difference between *not present* and *not visible* was made by using the contrast enhanced image; a ring not visible in the contrast enhanced image was considered as *not present*. The difference between *barely visible* and *visible* was subjective and based on sharpness appreciation. Images were displayed on a calibrated LCD screen with excellent colorimetric accuracy to optimize visual validation of the results. The compiled results are reported in Table I:

TABLE I
PERFORMANCE RESULTS OF OUR FLASH ARTIFACT DETECTOR

	Not present	**Not visible**	**Barely visible**	**Visible**
Ratios	25.53%	37.72%	35.41%	1.33%
Correct	90.94%	83.25%	90.20%	93.33%
Incorrect	9.06%	16.75 %	9.80%	6.67%
	Sensitivity	96.54%		
	Specificity	70.16%		

As one can see, the sensitivity of our approach is excellent but the specificity is average. About 75% of our images present a ring artifact. In those images, a ring artifact was detected each time and the *incorrect* rate corresponds to the inaccuracy in delineating the impacted area. For the remaining 25% of the images, the 9.06% error rate corresponds to the detection of a ring where none was present. This usually happened when the contrast enhanced image shows a large area that can attract the ring pattern used in the cross-correlation phase, therefore implying the presence of a ring. However, in future work, we expect to reduce this error rate, therefore improving the specificity, with a local colorimetric analysis.

V. CONCLUSION

We proposed a multi-steps morphological method to detect and to delineate annular flash artifacts located in the central region of fundus images. We justify our choice to use the combination of a colorimetric analysis and a morphological analysis instead of a usual probabilistic approach. We applied our method to a fairly large image database and obtained promising results, that will serve as basis for a next phase of flash artifact mitigation or local dedicated morphological analysis of the retina. In addition, the impact of the flash detection on automated screening performance will be evaluated in the near future.

REFERENCES

[1] Y. Li, T. P. Karnowski, K. W. Tobin, L. Giancardo, S. Morris, S. E. Sparrow, S. Garg, K. Fox, , and E. Chaum, "A health insurance portability and accountability actcompliant ocular telehealth network for the remote diagnosis and management of diabetic retinopathy," *Telemedicine and e-Health*, vol. 17, pp. 627–634, October 2011.

[2] L. Giancardo, M. D. Abramoff, E. Chaum, T. P. Karnowski, F. Meriaudeau, and K. W. Tobin, "Elliptical local vessel density: A fast and robust quality metric for retinal images," in *Engineering in Medicine and Biology Society, 2008. EMBS 2008. 30th Annual International Conference of the IEEE*, aug. 2008, pp. 3534 –3537.

[3] L. Giancardo, F. Meriaudeau, T. P. Karnowski, K. W. Tobin, Y. Li, and E. Chaum, "Microaneurysms detection with the radon cliff operator in retinal fundus images," B. M. Dawant and D. R. Haynor, Eds., vol. 7623, no. 1. SPIE, 2010, p. 76230U. [Online]. Available: http://link.aip.org/link/?PSI/7623/76230U/1

[4] L. Giancardo, F. Meriaudeau, T. P. Karnowski, Y. Li, S. Garg, K. W. T. Jr., and E. Chaum, "Exudate-based diabetic macular edema detection in fundus images using publicly available datasets," *Medical Image Analysis*, vol. 16, no. 1, pp. 216 – 226, 2012. [Online]. Available: http://www.sciencedirect.com/science/article/pii/S1361841511001010

[5] H. Santos-Villalobos, T. Karnowski, D. Aykac, L. Giancardo, Y. Li, T. Nichols, K. Tobin, and E. Chaum, "Statistical characterization and segmentation of drusen in fundus images," in *Engineering in Medicine and Biology Society, EMBC, 2011 Annual International Conference of the IEEE*, 30 2011-sept. 3 2011, pp. 6236 –6241.

[6] K. Fukunaga, *Introduction to Statistical Pattern Recognition*, 2nd ed. Academic Press, 1990.

[7] C. Hsin, H.-N. Le, and S.-J. Shin, "Color to grayscale transform preserving natural order of hues," in *Electrical Engineering and Informatics (ICEEI), 2011 International Conference on*, july 2011, pp. 1 –6.

[8] R. C. Gonzalez and R. E. Woods, *Digital Image Processing (3rd Edition)*. Upper Saddle River, NJ, USA: Prentice-Hall, Inc., 2006.

[9] M. Guizar-Sicairos, S. T. Thurman, and J. R. Fienup, "Efficient subpixel image registration algorithms," *Opt. Lett.*, vol. 33, no. 2, pp. 156–158, Jan 2008. [Online]. Available: http://ol.osa.org/abstract.cfm?URI=ol-33-2-156

[10] Z. Zhang, "Iterative point matching for registration of free-form curves and surfaces," *International Journal of Computer Vision*, vol. 13, pp. 119–152, 1994, 10.1007/BF01427149. [Online]. Available: http://dx.doi.org/10.1007/BF01427149

[11] D.-J. Kroon, "Iterative closest point using finite difference optimization to register 3d point clouds affine," 2009. [Online]. Available: http://www.mathworks.com/matlabcentral/fileexchange/24301